International Journal of Bio-Science and Bio-Technology
Vol.5, No.5 (2013), pp. 267-278
http://dx.doi.org/10.14257/ijbsbt.2013.5.5.26

An Analytical Solution for a Bio-heat Transfer Problem

Luisa Consiglieri

Independent Research Professor, 1600-256 Lisbon, European Union,
http://sites.google.com/site/luisaconsiglieri
lconsiglieri@gmail.com

Abstract

Catheter ablation along the posterior aspect of the left atrium has a small but real risk of esophageal perforation. This left atrioesophageal fistula formation is associated with multiple gaseous and/or septic embolic events causing cerebral and myocardial damage. The main objective is to mathematically model the ablation associated with delivery of radiofrequency (RF) energy to treat atrial fibrillation in order to control the temperature rise in the esophageal lumen. We model the heat exchange problem in a time-dependent multi-region for the catheter ablation therapy, with particular application to RF thermal ablation on the atrial tissue. From the selected set of geometric and operational parameters, benchmark calculations result in graphical representations. The proposed solutions enable whether quantitative or qualitative the study of temperature behavior whenever in space or in time. These enhance the physical understanding of what factors can affect the esophageal temperature and how to most accurately measure it. The model is sufficiently explicit to be, in turn, applied to different performances of one ablation procedure, or even to other thermal techniques.

Keywords: *Heat conduction; Analytical and numerical techniques*

1. Introduction

Thermal techniques to alter the abnormal conductive tissue generally fall into two categories: heat-based and cold-based procedures. The patients that are good candidates for one catheter-based ablation technique may not be for other type to have a chance at having their problem cured. Indeed, various energy sources have been used as the radiofrequency energy, the microwave, the laser, the cryothermia, and the high-intensity focused ultrasound [2, 13]. However, all procedures have one common involved risk: that of damage to nearby healthy tissue. The physiological problem is that the internal tissue temperature itself must be predicted. The main objective of this work is to improve thermal ablation technique by assuring exact calculations of the temperature. The established bio-heat transfer problem consists of an initial-boundary value problem to a system of parabolic equations, in coupled physiologically distinct regions. An accurate heat transfer model in blood perfused tissues can contribute to reduce treatment time, to control the size of the coagulative necrosis, and to predict the better geometry of the ablation setup.

Over the past decade, a large number of modeling approaches aimed at elucidating the radio-frequency (RF) ablation which is the technique that applies hyperthermia through electrical current in order to destroy portions of tissue and causes a scar in that region [5, 20, 19, 24]. As cardiac application, cells lose electrical excitability and the reentrant pathways are interrupted. Then the scar tissue cannot transmit electrical impulses, and the abnormal electrical pathway may no longer be able to generate cardiac arrhythmias [8, 25]. Thus, the

ISSN: 2233-7849 IJBSBT

RF ablation procedure can also permanently cure atrioventricular nodal reentrant tachycardia, atrial fibrillation, accessory pathway mediated tachycardia, atrial flutter, atrial tachycardia or idiopathic ventricular tachycardia [15].

Experimental studies have revealed that during percutaneous RF ablation, damage can occur in the lungs, phrenic nerves, and pulmonary venous tissue [2]. The most significant complication of left atrium (LA) catheter ablation is atrioesophageal fistula formation. This complication (although rare) is associated with significant mortality and morbidity, including air embolism, sepsis, endocarditis, and gastrointestinal exsanguination [11]. Possible clinical solutions include development of real-time esophageal location, temperature monitoring, the use of lower-power or alternative energy sources when ablation near the esophagus is necessary, and improved early detection of esophageal injury [22, 26]. The esophageal injuries occur with unipolar radiofrequency and microwave energies [16].

Numerical studies have been focused upon the prediction of lesion formation, as well as, the heat transfer effects on lesion dimension during the treatment (see [12, 17, 35] and the references therein). In those works the problem under study has been solved by means of finite element method, and the existence of solution was not proved. In [14], an exact solution is obtained by the successive application of the methods of superposition, separation of variables and multi-region Green's function. Previous exact solutions introduced by [3] had made the rather limiting assumptions that the domain of the model is defined as two concentric spherical regions, the inner representing the diseased tissue and the outer the healthy tissue. Hence, the heat equation is only dependent on one radial direction, i.e. the physiological material exhibits a 1D behavior.

In this work, we present an analytical temperature solution for the zone of active heating from the LA posterior wall to the esophagus during the RF cardiac catheter ablation. Two different positions of the ablating electrodes are considered: (1) one ablating electrode placed on the endocardium; and (2) two ablating electrodes equidistantly placed on the endocardial interface from the one of case 1. To this end, we respectively propose two analytical solutions to the bio-heat transfer problem in sagittal multi-region. To evaluate the high temperatures that arrive near the esophagus is of particular concern in order to avoid damage to the esophagus. Therefore, the present formulated problem plays a crucial role in preventing the cascade of events that eventually result in the development of LA-Eso fistula.

Specific physiological measurements are not made during the study. Anthropometric measurements are selected from the literature to enable the numerical simulations. The closed-form solutions are computationally evaluated. The theoretical predictions agree with previously reported findings. The development of physiologically accurate, yet mathematically rigorous theoretical models may lead to an improvement in predictive capability.

Next section briefly outlines the cardiac catheter ablation model, directional catheters at the endocardial approach, and the framework that incorporates the heat transfer. Having described the model itself, attention is next focused upon the utilization of the model for a particular multi-region in Section 2.1. In Section 3, the assumptions on the data are stated. Section 4 is devoted to a few, but relevant, different numerical simulations, and identifying the main results. The paper concludes with offering directions for future model development and study. An analytical solution is determined in Appendix.

2. Cardiac Catheter Ablation

The heart consists of two pumps (the right and the left) connected in series that pump blood through the circulatory system. The left ventricle is a thick-walled body composed of

myocardium between a thin outer membrane (epicardium) and an inner membrane (endocardium); and receives the most attention in the literature because most infarcts occur in this chamber. The hyperthermia technique consists of placing the ablating electrodes into a heart chamber via percutaneous peripheral venous or arterial conduits and of placing an indifferent electrode on the skin at the back of the patient. Current is applied between each catheter electrode and the ground one creating an electromagnetic field. Then by ionic agitation, electromagnetic energy is transformed into heat, causing tissue dehydration, and irreversible injury occurs. In this study, we take into account two different positions of the ablating electrodes: (case 1) one thin electrode is placed in perpendicular contact with the endocardium; and (case 2) two electrodes (or one umbrella electrode) are placed parallel to each other at a close distance in order to create a similar situation to the ideal case of two parallel plates.

Although at the initial instant of time (t = 0 s) only a thin rim of tissue adjacent to the catheter tip is heated by the Joule effect and heat conduction, and the surrounding region is mainly heated by the conduction from above region, there exists an instant of time t_0 such that the electric current flow through the tissue causes resistive heating (Joule effect) of a small three dimensional domain. For the sake of simplicity t_0 = 0 is assumed. Let Ω be the 3D domain such that its sagittal cross-section being of the rectangular form]0,L[×]0,H[with L and H denoting the total distance between the endocardial surface of the LA and midesophagus lumen and the height of the heated region, respectively (see Figures 1 and 2). The zone of active heating caused by RF ablation has a controlled size in order to protect the healthy cells.

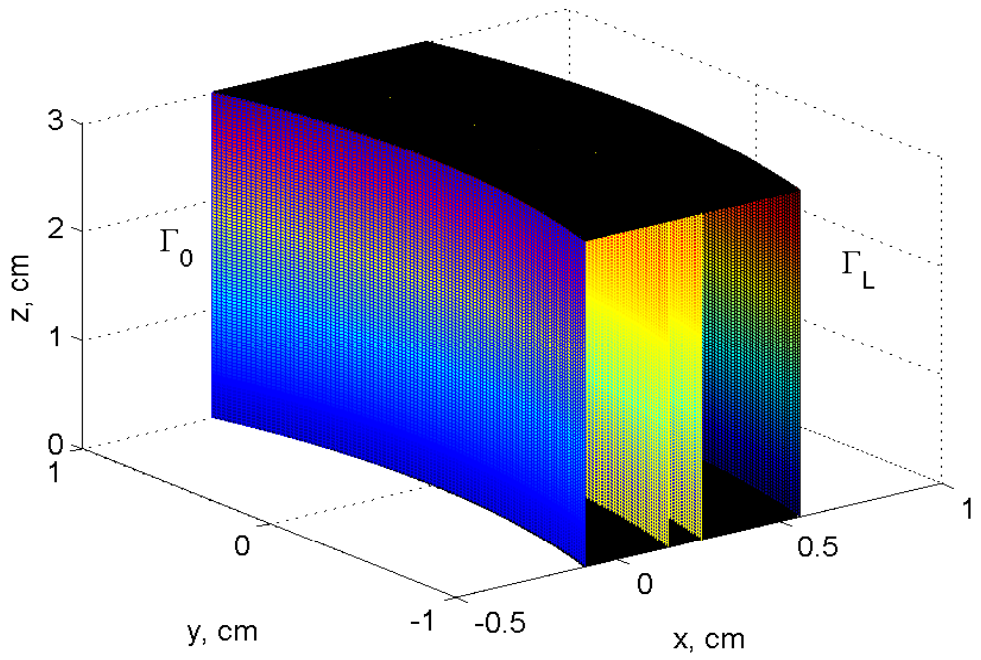

Figure 1. Schematic Representation of the Domain, where the Inner surface Γ_0 Represents the Endocardial Surface in Contact with the Blood in the Heart Chamber, and the Outer Surface Γ_L Represents the Esophageal Surface in Contact with the Air

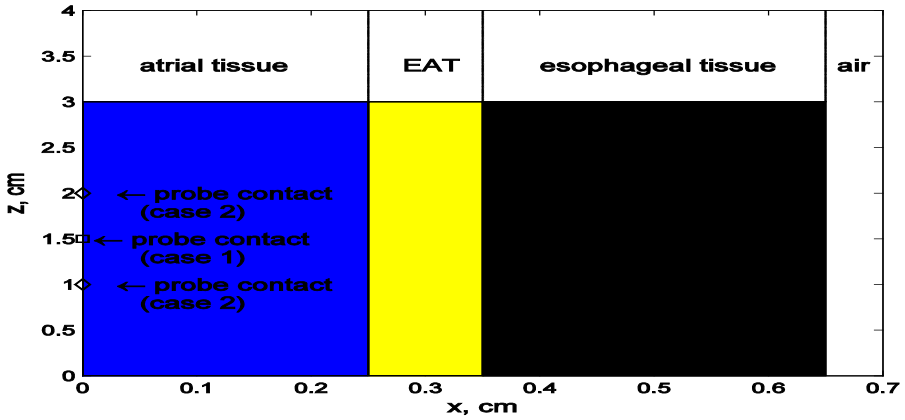

Figure 2. Schematic Representation of the Sagittal Cross-sectioned Domain in the Plane Oxz

The bio-heat transfer problem is constituted by the Pennes' bioheat equation [28], in the domain Ω,

$$\rho c\, \partial_t T = k\Delta T + \mathbf{J}\bullet\mathbf{E} - \rho_b c_b w\,(T - T_b) + Q_m\,, \qquad (1)$$

where T is the temperature, ρ is the density, c is the specific heat capacity per unit mass, k is the thermal conductivity, T_b represents the temperature of the blood (assumed to be 38 °C) and ρ_b, c_b, and w denote the density, the specific heat capacity, and the volumetric flow of the blood, respectively. Moreover, $\omega = \rho_b w$ (kg•m^{-3}•s^{-1}), represents the blood perfusion that occurs in the capillary bed, and $c_b\omega$ accounts for the heat conducted in direction of the contribution of flowing blood to the overall energy balance, i.e. the energy exchange by the flowing blood was modeled as a non-dimensional (non-directional) heat source [1, 23]. The perfusion ceases ($w = 0$) whenever the concentration c of living cells verifies $c(t) \leq c(0)\exp[-1]$. This corresponds to $\Omega(t) \geq 1$, with Ω being the degree of tissue injury such that, at each instant of time, the cumulative damage integral is computed using the Arrhenius equation [9]

$$\Omega(t)=\ln[c(0)/c(t)]= A\int^t \exp[-(RT(\tau))^{-1}E]\, d\tau, \qquad (2)$$

where R is the universal gas constant, A is a frequency factor, and E is the activation energy for the irreversible damage reaction.

The left-hand side of (1) represents the heat accumulated within the tissue control volume. On the right-hand side of the Pennes' equation, the term **J•E** represents the power density p of the electromagnetic field, which is converted into thermal energy, with **J** and **E** being the current density and the electric field intensity, respectively. Finally, the energy generated by the metabolic processes Q_m can be neglected, *i.e.*, $Q_m = 0$ W•m^{-3}.

The existence of on one side the blood and on other side the air near the heated tissue implies that heat is carried away from that heated zone. This heat exchange at the blood-tissue and air-tissue interfaces reads

$$-k\,\nabla T\bullet\mathbf{n} = h\,(T - T_b) \qquad \text{on} \quad \Gamma_0 \quad \text{(inner surface);} \qquad (3)$$

$$-k\,\nabla T\bullet\mathbf{n} = h_L\,(T - T_{air}) \qquad \text{on} \quad \Gamma_L \quad \text{(outer surface),} \qquad (4)$$

where h_L is the heat transfer coefficient accounting for the esophageal lumen, and T_{air} represents the temperature of the air in the esophagus canal (assumed to be 36.2 °C, the baseline esophagus luminal temperature in [11]). The endocardial convective heat transfer coefficient h is known [33]. The no outflow is assumed

$$k\ \nabla T \bullet \mathbf{n} = 0 \qquad \text{on} \qquad \Gamma := \text{int}(\partial\Omega \backslash (\Gamma_0 \cup \Gamma_L)). \tag{5}$$

A few comments should be added regarding to the domain. The domain is the multi-region constituted by the posterior wall of the LA from endocardium to epicardium, the fatty tissue, and the esophageal wall adjacent to the posterior LA that is constituted by muscular, submucosal and mucosal layers together [30]. Then $L = L_a + L_f + L_e$, where L_a, L_f and L_e denote the thickness of atrial wall, fat pad and esophageal wall, respectively, and there are three subdomains, namely atrial, fat and esophageal (see Table 1, and Figures 1 and 2).

Table 1. Physiological Parameters [18]

	blood	atrial wall	fat pad	esophageal wall
L (mm)		2.5	1.0	3.0
k (W•m^{-1}• °C^{-1})	0.52	0.53	0.21	0.56
ρ (kg• m^{-3})	1060	1080	910	1040
c (J•kg^{-1}• °C^{-1})	3600	3690	2350	3500
w (kg•m^{-3}• s^{-1})		1	0	0.2

2.1. The Mathematical Model

In order to find exact solutions for the temperature let us consider some finite time $t_* > 0$, and an annular domain

$$\Omega = \{(x,y,z) \in \mathbb{R} \times]-W/2, W/2[\times]0, H[: \ r^2 < (x + r)^2 + y^2 < (r + L)^2\},$$

with L, W, H, $r > 0$ stand for the length, width, height, and inner radius, respectively. Hereafter, the subscripts a, f and e stand for the atrial, fat and esophageal designations, respectively. In particular, set

$$\Omega_a = \{(x,y,z) \in \Omega : \ r^2 < (x + r)^2 + y^2 < (r + L_a)^2\},$$

$$\Omega_f = \{(x,y,z) \in \Omega : \ (r + L_a)^2 < (x + r)^2 + y^2 < (r + L_w)^2\},$$

$$\Omega_e = \{(x,y,z) \in \Omega : \ (r + L_w)^2 < (x + r)^2 + y^2 < (r + L)^2\},$$

where $L_w = L_a + L_f$. The model in the multi-region domain reads

$$\rho_a c_a \partial_t T_a = k_a \Delta T_a + \mathbf{J} \bullet \mathbf{E} - c_b \omega_a (T_a - T_b), \qquad \text{in} \quad \Omega_a \times]0, t_*[; \tag{6}$$

$$\rho_f c_f \partial_t T_f = k_f \Delta T_f + \mathbf{J} \bullet \mathbf{E}, \qquad \text{in} \quad \Omega_f \times]0, t_*[; \tag{7}$$

$$\rho_e c_e \partial_t T_e = k_e \Delta T_e + \mathbf{J} \bullet \mathbf{E} - c_b \omega_e (T_e - T_b), \qquad \text{in} \quad \Omega_e \times]0, t_*[. \tag{8}$$

Since the main thermal equilibration process that takes place in the fatty pad, Ω_f , does not account for the capillaries, we use the heat equation instead of the Pennes' bioheat equation.

In cylindrical coordinates, (6)-(8) read as follow:

$$\rho_i c_i \partial_t T_i = k_a (\partial_\rho^2 T_i + \rho^{-1} \partial_\rho T_i + \rho^{-2} \partial_\theta^2 T_i + \partial_z^2 T_i) + \mathbf{J} \bullet \mathbf{E} - c_b \omega_i (T_i - T_b),$$

$$\rho_f c_f \partial_t T_f = k_f \ (\partial_\rho{}^2 T_f + \rho^{-1} \partial_\rho T_f \ + \rho^{-2} \ \partial_\theta{}^2 T_f + \partial_z{}^2 T_f) \ + \mathbf{J}\bullet\mathbf{E},$$

for all $(\rho,\theta,z,t) \in]r,r+L[\times]\arcsin(-W/(2\rho)),\arcsin(W/(2\rho))[\times]0,H[\times]0,t_*[$, and i=a,e. The heat transfer mechanisms (3)-(4) read, respectively,

$$-k_a \partial_\rho T_a = h\,(T_a - T_b) \qquad \text{if} \quad \rho = r, \tag{9}$$

$$k_e \partial_\rho T_e = h_L\,(T_e - T_{air}) \qquad \text{if} \quad \rho = r + L, \tag{10}$$

for any $(\theta,z,t) \in]\arcsin(-W/(2\rho)),\arcsin(W/(2\rho))[\times]0,H[\times]0,t_*[$. Here the coefficient h_L is unknown. The continuity conditions are at the atrial-fat and wall of the esophagus interfaces ($L_a = \partial\Omega_a \cap \partial\Omega_f$, and $L_w = \partial\Omega_f \cap \partial\Omega_e$), respectively,

$$T_f = T_i, \qquad k_f \partial_x T_f = k_i \partial_x T_i \qquad \text{for} \quad i = a, e. \tag{11}$$

The noflux boundary condition (5) reads

$$\partial_z T_a = \partial_z T_f = \partial_z T_e = 0 \qquad \text{if} \quad z = 0, H; \tag{12}$$

$$\partial_\theta T_a = \partial_\theta T_f = \partial_\theta T_e = 0 \qquad \text{if} \quad \rho \sin(\theta) = \pm W/2,$$

for any $(\rho,z,t) \in]r,r+L[\times]0,H[\times]0,t_*[$.

The initial condition is such that T reaches its maximum with value of T_1, at the exact positions of the electrodes. Here, we consider $z = H/\kappa$, and $z = (\kappa - 1)H/\kappa$, with $\kappa = 2$ (case 1), and $\kappa = 3$ (case 2).

This boundary value problem to the bio-heat transfer system (6)-(8) admits the 2D solution established in Appendix.

9. Method

In the simulations carried out here, the physiological values are in accordance with Table 1. Among the clinical variables of age, sex, body weight, and LA size, there are no independent predictors of the presence or thickness of the fat pad between the esophagus and the posterior LA nor spatial relations of the thickness of the posterior atrial wall [21]. The position of the esophagus relative to the LA varies considerably between patients and varies even in a single patient during an ablation procedure. The cross-sectioned fatty pad is assumed 1 mm thick [21]. Additionally, the mean thickness of the posterior LA wall ranges from 1.9 to 4.0 mm, and the mean thickness of the esophageal wall (from mucosa to adventitia) adjacent to the LA ranges from 1.5 to 4.5 mm [2, 11, 30]. In the presence of these factors, we take average values for the physiological parameters in Table 1.

Here RF energy is applied initially at 23 W, the power is titrated up in 2-W increments every 5 seconds to a maximum of 35 W, in accordance with that the current clinical strategy to minimize esophageal thermal injury during AF ablation involves limiting the magnitude of power (25 to 35 W), as well as the duration (<30 s), of RF applications placed along the posterior wall of the LA [31]. Joule heating arises when energy dissipated by the electric current flowing through the conductor is converted into thermal energy [34].

We impose the blood perfusion parameters for the atrial and the esophageal tissues to be both constant, since there is no coagulation zone beyond the time $t = 30$ s. Indeed, $\Omega(t) < 1$ for all $t \in]0,30[$, considering that (2) implies

$$\forall\, t \in]0,30[\quad \Omega(t) \leq \Omega(30) \leq 30A\exp[-E\,(RT(x,z,30))^{-1}] < 1,$$

for temperatures $T(x,z,30) < E/(R \ln[30A]) \simeq 58$ °C under values for the atrial tissue, $A = 2.94\times 10^{39}\ s^{-1}$ and $E = 2.596\times 10^{5}\ J\bullet mol^{-1}$ [27].

4. Results and Discussion

The simulations displayed in Figure 3 correspond to x = 0 and x = L (*i.e.*, the functions z → T_a (0,z,0) and z → T_e (L,z,0) in accordance with Appendix). Figure 3 indicates the discrepancy between the two shapes, which is attributed to the different positions of the electrodes. The temperature has its maximum values at the point (x,z) = (0,H/2) in case 1 and at the points (x,z) = (0,H/3) and (x,z) = (0,2H/3) in case 2 which coincide with the locations at the endocardial surface of the target ablation region where the catheters are placed. These mean that the electrodes create a distribution of temperature that is large only under the electrode(s). Their shape is maintained over time, it is the amplitude that is strongly reduced. The temperature T_e has reduced amplitude along the esophagus course as monitored in [11].

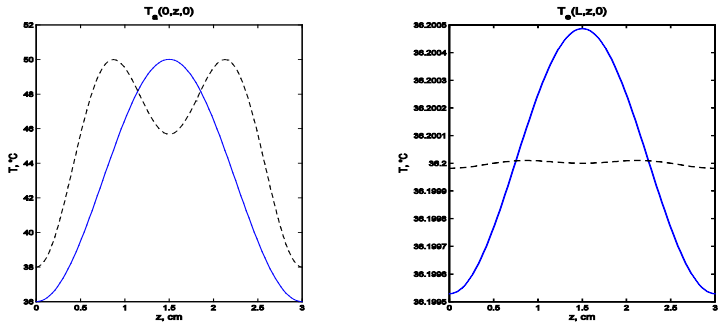

Figure 3. Graphical Representation of the Temperature versus the Height Distance z. Case 1: Solid Lines. Case 2: Dashed Lines

Figure 4 displays the solution to (6)-(12) for cases 1 and 2, respectively in (a) and (b), at the instant of time t =30 s, plotted against the sagittal region]0,L[×]0,H[, with $L = 6.5\times 10^{-1}$ cm denoting the total distance between the blood and the air, and H = 3 cm the height of the heated region. Their configurations almost coincide, which does not afford relevant information about one ideal position of the electrode. However, this agreement confirms that the temperature stabilizes with time as recorded in [7].

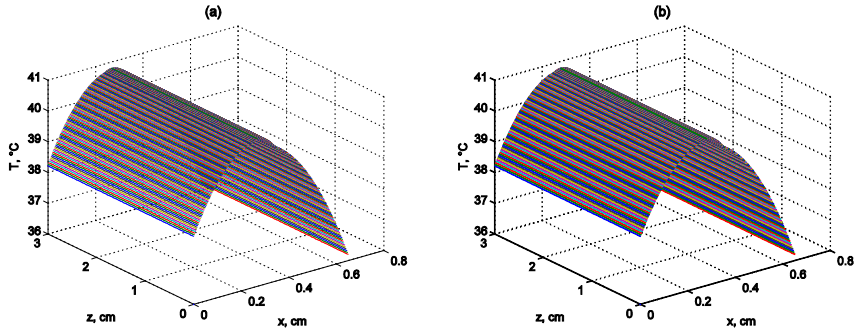

Figure 4. Graphical Representation of the Temperature versus the Sagittal Domain in the Plane Oxz, at Power Output of 35 W: (a) when one Electrode is taken into Account (case 1); (b) when Two Electrodes are Taken into Account (case 2)

In the both modalities, T first increases and next decreases as a function of distance from the catheter surface. Its maximum is not attained at the boundary but it is reached ≈ 3 mm from the ablating electrodes, which agrees with the experimental findings in [6]. This is consistent with the so-called blood cooling effect. This effect acts as an additional dissipation due to the higher electrical conductivity of the blood. We remark that the electric field intensity **E** can be expressed as $\mathbf{E} = \mathbf{J}/\sigma$, where σ is the electrical conductivity, then $p = \sigma|\mathbf{E}|^2$. Indeed, there are two collateral effects: the proximity of the blood flow rate to the probe, and the blood perfusion term in the Pennes' bioheat equation.

The results of the previous simulations clarify how the model can be used to suggest additional experimental studies in order to help, justify, or refute various model assumptions.

5. Conclusions

A simple 2D analytical solution that solves the bio-heat transfer problem is established. This proposed solution accounts for the variability in the thickness of the posterior LA wall and the presence of periesophageal connective tissue: factors that potentiate the esophageal injury. Indeed, all local properties of the ablation site can easily be changed in the present mathematical model as per each ablation. Such minor changes can have impact upon transport issues. For instance, the mathematical model reveals that L_f contributes to diminish the temperature along the esophageal course. This agrees with the interpretation that L_a and L_f, in very thin persons, are one of the concerns of the surgeons [16].

The major contribution of the solution is that it is sufficiently explicit (cf. Appendix) to be, in turn, applied to different performances of one ablation procedure, or even to other thermal techniques. In addition, the dependence of the temperature as function of RF power delivery during AF ablation, and of duration of RF applications, is other of the upgrades. Since the data are of extreme importance on the convergence tests in numerical methods (see [4, 10] and the references therein), the presented solution maybe a tool before getting into highly detailed and more anatomically appropriate numerical models to design therapy. Moreover, it allows a quantitative study.

In conclusion, the model presents several advantages: (1) its simplicity; (2) its capacity to perform a large range of different simulations; (3) the possibility of qualitatively studying the effect of different geometric and operational parameters; and (4) its negligible computational cost.

In the sequence of our achievements, the following developments remain as open problems to be studied in the future. First, seek an analytical solution with the dependence of the myocardial conductivity on the temperature via the Kirchhoff transformation applied to the Pennes' bioheat equation. In particular, k_a increases if the temperature increases. Thus, it raises the temperature (in other regions) and causes a larger boundary lesion. The excessive temperature results in dehydrated tissue. The dehydrated myocardium is both an electrical and thermal insulator. Therefore, safety requires that the depth of tissue injury must be controlled during ablation and the delivery of energy must be directed to avoid collateral damages.

Finally, extend the model to a new one defined on a domain that includes a small volume of the blood pool in the cardiac chamber, where the Pennes' bioheat equation is replaced by the heat advection-diffusion equation instead of using the Newton's law of cooling at the blood-tissue interface with h being assumed constant.

6. Appendix

The power is assumed constant, uniform in space and in time over every interval of 5 seconds, as mentioned in Section 3. Thus, for each interval of time $]5i,5(i+1)[$ $(i = 0,\bullet\bullet\bullet,5)$ we

seek one analytical solution of (6)-(8). For the sake of simplicity in notations, we will omit the index i, keeping in mind that **J** • **E** corresponds to a well-determined interval of time. We find the atrial, fat and esophageal temperatures, adapting the Fourier method of separation of variables [29], as

$T_a(x,z,t) = a_0 \cos(a_1 x + a_2) \cos(a_3 z + a_4) \exp(a_5 t) + a_6 \exp(a_7 x) + a_8 \exp(-a_7 x) + a_9$;

$T_f(x,z,t) = b_0 \cos(b_1 x + b_2) \cos(b_3 z + b_4) \exp(b_5 t) + b_6 x^2 + b_7 x + b_8$;

$T_e(x,z,t) = c_0 \cos(c_1 x + c_2) \cos(c_3 z + c_4) \exp(c_5 t) + c_6 \exp(c_7 x) + c_8 \exp(-c_7 x) + c_9$.

Notice that some other forms of solutions of PDE clearly do not fulfill the transmission, boundary, and initial conditions. Indeed, it is upon the presence of our transmission, boundary, and initial conditions, that the choice of the above functions is suitable for the mathematical model. That is, they are solutions to (6)-(8) considering that the constants a_1, a_2, a_5, a_7, a_9, b_1, b_3, b_5, b_6, c_1, c_2, c_5, c_7, c_9 satisfy

$$\rho_a c_a a_5 = -k_a (a_1^2 + a_3^2) - c_b \omega_a, \qquad a_7^2 = c_b \omega_a / k_a, \qquad a_9 = T_b + (c_b \omega_a)^{-1} \mathbf{J} \cdot \mathbf{E}; \tag{13}$$

$$\rho_f c_f b_5 = -k_f (b_1^2 + b_3^2), \qquad b_6 = -(2k_f)^{-1} \mathbf{J} \cdot \mathbf{E}; \tag{14}$$

$$\rho_e c_e c_5 = -k_e (c_1^2 + c_3^2) - c_b \omega_e, \qquad c_7^2 = c_b \omega_e / k_e, \qquad c_9 = T_b + (c_b \omega_e)^{-1} \mathbf{J} \cdot \mathbf{E}. \tag{15}$$

From (9) and using (13) it follows that

$$a_2 = \arctan[-h(k_a a_1)^{-1}], \qquad (k_a c_b \omega_a)^{1/2} (a_6 - a_8) = h(a_6 + a_8 + (c_b \omega_a)^{-1} \mathbf{J} \cdot \mathbf{E}).$$

From (11) it follows that

$$a_i = b_i = c_i \qquad (i = 3,4,5); \tag{16}$$

$a_0 \cos(a_1 L_a + a_2) = b_0 \cos(b_1 L_a + b_2)$;

$a_6 \exp(a_7 L_a) + a_8 \exp(-a_7 L_a) + a_9 = b_6 L_a^2 + b_7 L_a + b_8$;

$k_a a_0 a_1 \sin(a_1 L_a + a_2) = k_f b_0 b_1 \sin(b_1 L_a + b_2)$;

$k_a a_7 (a_6 \exp(a_7 L_a) - a_8 \exp(-a_7 L_a)) = k_f (2 b_6 L_a + b_7)$;

$c_0 \cos(c_1 L_w + c_2) = b_0 \cos(b_1 L_w + b_2)$;

$c_6 \exp(c_7 L_w) + c_8 \exp(-c_7 L_w) + c_9 = b_6 L_w^2 + b_7 L_w + b_8$;

$k_e c_0 c_1 \sin(c_1 L_w + c_2) = k_f b_0 b_1 \sin(b_1 L_w + b_2)$;

$k_e c_7 (c_6 \exp(c_7 L_w) - c_8 \exp(-c_7 L_w)) = k_f (2 b_6 L_w + b_7)$.

Thus, using (13)-(15) and (16) it follows that

$$(k_a (a_1^2 + a_3^2) - c_b \omega_a) (\rho_a c_a)^{-1} = k_f (b_1^2 + a_3^2) (\rho_f c_f)^{-1} = (k_e (c_1^2 + a_3^2) - c_b \omega_e) (\rho_e c_e)^{-1}.$$

From (10) it follows that

$k_e c_1 \tan(c_1 L + c2) = h_L$,

$-k_e c_7 (c_6 \exp(c_7 L) - c_8 \exp(-c_7 L)) = h_L (c_6 \exp(c_7 L) + c_8 \exp(-c_7 L) + c_9 - T_{air})$.

The initial condition at the catheter-tissue electrode interface is

case 1: $\cos(a_3 H/2 + a_4) = 1$, and $T_a(0, H/2, 0) = T_1$, *i.e.*,

$$a_0 \cos(a_2) + a_6 + a_8 + a_9 = T_1,$$

with an initial temperature T_1 =50 °C. Moreover, (12) is solved by

$$a_3 = b_3 = c_3 = 2\pi/H, \qquad a_4 = b_4 = c_4 = -\pi.$$

case 2: $T_a\,(0,H/3,0) = T_a\,(0,2H/3,0) = T_1$, and

$$a_{3,1}\sin(a_{3,1}H/3 + a_{4,1}) + a_{3,2}\sin(a_{3,2}H/3 + a_{4,2}) = 0;$$
$$a_{3,1}\sin(a_{3,1}2H/3 + a_{4,1}) + a_{3,2}\sin(a_{3,2}2H/3 + a_{4,2}) = 0.$$

From (12) it follows that

$$a_{3,1}\sin(a_{4,1}) + a_{3,2}\sin(a_{4,2}) = 0;$$
$$a_{3,1}\sin(a_{3,1}H + a_{4,1}) + a_{3,2}\sin(a_{3,2}H + a_{4,2}) = 0.$$

Therefore, we may take

$$a_{3,1} = 2\pi/H, \qquad a_{3,2} = 4\pi/H, \qquad a_{4,1} = a_{4,2} = -\pi.$$

Finally, $T_e\,(L,0,0) = T_e\,(L,H,0) = T_{air}$ implies

$$c_0\cos(c_1L + c_2)\cos(\pm\pi) + c_6\exp(c_7L) + c_8\exp(-c_7L) + c_9 = T_{air}.$$

Note that the constants a_3, a_4, a_7, a_9, b_3, b_4, b_6, c_3, c_4, c_7, c_9 can be calculated directly from the data. Observe that (17) yields b_1 and c_1 in function of a_1. The remaining constants (including h_L) are well determined since they solve the remaining equations (a system of 17 equations).

References

[1] H. Arkin, L. X. Xu and K. R. Holmes, IEEE Trans. Biomed. Eng., vol. 41, no. 2, **(1994)**, pp. 97.
[2] H. Aupperle, N. Doll, T. Walther, P. Kornherr, C. Ullmann, H.-A. Schoon and F. W. Mohr, J. Thorac. Cardiovasc. Surg., vol. 130, **(2005)**, pp. 1549.
[3] H. G. Bagaria and D. T. Johnson, Int. J. Hyperthermia, vol. 21, no. 1, **(2005)**, pp. 57.
[4] E. J. Berjano, BioMedical Engineering Online, vol. 5, **(2006)**, pp. 24.
[5] E. Bugge, I. A. Nicholson and S. P. Thomas, Eur. J. Cardiothorac. Surg., vol. 28, **(2005)**, pp. 76.
[6] F. Burdío, E. J. Berjano, A. Navarro, J. M. Burdío, A. Guemes, L. Grande, R. Sousa, J. Subiró, A. Gonzalez, I. Cruz, T. Castiella, E. Tejero, R. Lozano and M. A. Gregorio, BioMedical Engineering Online, vol. 6, **(2007)**, pp. 30.
[7] H. Cao, V. R. Vorperian, S. Tungjitkusolmun, J.-Z. Tsai, D. Haemmerich, Y. B. Choy and J. G. Webster, IEEE Trans. Biomed. Eng., vol. 48, no. 4, **(2001)**, pp. 425.
[8] R. Cappato, H. Calkins, S.-A. Chen, W. Davies, Y. Iesaka, J. Kalman, Y.-H. Kim, G. Klein, D. Packer and A. Skanes, Circulation, vol. 111, **(2005)**, pp. 1100.
[9] I. A. Chang and U. D. Nguyen, BioMedical Engineering Online, vol. 3, **(2004)**, pp. 27.
[10] C. C. Chen, M. I. Miga and R. L. Galloway, Med. Phys., vol. 34, no. 10, **(2007)**, pp. 4030.
[11] J. E. Cummings, R. A. Schweikert, W. I. Saliba, J. D. Burkhardt, J. Brachmann, J. Gunther, V. Schibgilla, A. Verma, M. Dery, J. L. Drago, F. Kilicaslan and A. Natale, Circulation, vol. 112, **(2005)**, pp. 450.
[12] N. Doll, M. A. Borger, A. Fabricius, S. Stephan, J. Gummert, F. W. Mohr, J. Hauss, H. Kottkamp and G. Hindricks, J. Cardiovasc. Surg., vol. 125, **(2003)**, pp. 836.
[13] J. Dunning, M. Nagendran, O. R. Alfieri, S. Elia, A. P. Kappetein, U. Lockowandt, G. E. Sarris and P. H. Kolh, Eur. J. Cardiothorac. Surg., vol. 44, no. 5, **(2013)**, pp. 777.
[14] J. W. Durkee Jr. and P. P. Antich, Phys. Med. Biol., vol. 36, no. 3, **(1991)**, pp. 345.
[15] R. E. Eckart and L. M. Epstein, Cardiac Surgery in the Adult, Edited L. H. Cohn, McGraw-Hill, NewYork **(2008)**, pp. 1357-1374.
[16] A. M. Gillinov, G. Pettersson and T. W. Rice, J. Thorac. Cardiovasc. Surg., vol. 122, **(2001)**, pp. 1239.
[17] J. Gopalakrishnan, Annals of Biomedical Engineering, vol. 30, **(2002)**, pp. 884.
[18] P. A. Hasgall, E. Neufeld, M. C. Gosselin, A. Klingenbock and N. Kuster, "IT'IS Database for thermal and electromagnetic parameters of biological tissues", Version 2.2, July 11th, 2012. www.itis.ethz.ch/database.
[19] S. Jacobsen and P. R. Stauffer, Phys. Med. Biol., vol. 52, no. 4, **(2007)**, pp. 911.
[20] Z. Kaouk, A. V. Shahidi, P. Savard and F. Molin, Med. Biol. Eng. Comput., vol. 34, **(1996)**, pp. 165.
[21] K. Lemola, M. Sneider, B. Desjardins, I. Case, J. Han, E. Good, K. Tamirisa, A. Tsemo, A. Chugh, F. Bogum, F. Pelosi, E. Kazerooni, F. Morady and H. Oral, Circulation, vol. 110, **(2004)**, pp. 3655.

[22] E. Liu, M. Shehata, T. Liu, A. Amorn, E. Cingolani, V. Kannarkat, S. S. Chugh and X. Wang, Journal of Interventional Cardiac Electrophysiology, vol. 35, no. 1, **(2012)**, pp. 35.
[23] G. T. Martin and H. F. Bowman, Med. Biol. Eng. Comput., vol. 38, **(2000)**, pp. 319.
[24] E. S. McCreedy, R. Cheng, P. F. Hemler, A. Viswanathan, B. J. Wood and M. J. McAuliffe, IEEE Transactions on Information Technology in Biomedicine, vol. 10, no. 3, **(2006)**, pp. 490.
[25] K. Nademanee, J. McKenzie, E. Kosar, M. Schwab, B. Sunsaneewitayakul, T. Vasavakul, C. Khunnawat and T. Ngarmukos, J. Am. Coll. Cardiol., vol. 43, no. 11, **(2004)**, pp. 2044.
[26] M. D. O'Neill, P. Jais, M. Hocini, F. Sacher, G. J. Klein, J. Clémenty and M. Hassaiguerre, Circulation, vol. 116, **(2007)**, pp. 1515.
[27] J. A. Pearce, Proc. SPIE 7181 **(2009)**, 718104 p.15.
[28] H. H. Pennes, J. Applied Physiology, vol. 1, no. 2, **(1948)**, pp. 93.
[29] A. D. Polyanin, "Handbook of linear partial differential equations for engineers and scientists" Chapman & Hall/CRC", Boca Raton, **(2002)**.
[30] D. Sánchez-Quintana, J. A. Cabrera, V. Climent, J. Farré, M. C. Mendonça and S. Y. Ho, Circulation, vol. 112, **(2005)**, pp. 1400.
[31] S. M. Singh, A. d'Avila, S. K. Doshi, W. R. Brugge, R. A. Bedford, T. Mela, J. N. Ruskin and V. Y. Reddy, Circulation, vol. 1, **(2008)**, pp. 162.
[32] E. Sparrow and J. Abraham, Annals of Biomedical Engineering, vol. 36, **(2008)**, pp. 171.
[33] C. Tangwongsan, J. A. Will, J. G. Webster, K. L. Meredith Jr. and D. M. Mahvi, IEEE Trans. Biomed. Eng., vol. 51, **(2004)**, pp. 1478.
[34] S. Tungjitkusolmun, E. J. Woo, H. Cao, J.-Z. Tsai, V. R. Vorperian and J. G. Webster, Med. Biol. Eng. Comput., vol. 38, **(2000)**, pp. 562.
[35] R. Weerasooriya, P. Khairy, J. Litalien, L. Macle, M. Hocini, F. Sacher, N. Lellouche, S. Knecht, M. Wright, I. Nault, S. Miyazaki, C. Scavee, J. Clementy, M. Haissaguerre, P. Jais, J. Am. Coll. Cardiol., vol. 57, **(2011)**, pp. 160.

Authors

Luisa Consiglieri, she received her B.S., M.S. and Ph.D. degrees in mathematics from University of Lisbon in 1988, 1992 and 2000, respectively. She taught at the Faculty of Sciences of University of Lisbon from 1987 until her retirement (by speech disorder) in April 2009. Her research interests are related to the classical questions in Partial Differential Equations (PDE) theory, i.e. the existence, uniqueness and regularity of solutions of initial-boundary value problems. The research interests span a variety of areas in differential equations such as continuum mechanics: in particular fluid mechanics, heat transfer, and electromagnetism. At the present, her principal aim is the crossdisciplinarity (which includes multi-, inter-, and transdisciplinary) involving chemistry, geophysics, medical biophysics, and biomedical engineering: with emphasis in biomechanics.